Comparison of Two Kinds of Functionally Graded Conical Shells with Various Gradient Index for Vibration Analysis

Amirhossein Nezhadi*, Roslan Abdul Rahman, Amran Ayob
Faculty of Mechanical Engineering, Universiti Teknologi Malaysia (UTM), 81310 Skudai, Johor, Malaysia
*E-mail: a_h_nezhadi@yahoo.com

Abstract: In this paper, a study on the effects of the FGM configuration is taken into account by studying the frequencies of two FG conical shells. Type I FG conical shell has aluminum on its inner surface and almina on its outer surface and Type II FG cylindrical shell has almina on its inner surface and aluminum on its outer surface. The study is done based on Rayleigh-Ritz method. The objective is to study the effects of configurations of the constituent materials on the frequencies. The properties are graded in the thickness direction according to the gradient index distribution. The analysis is carried out with strains-displacement relations are given by Soedel (1981). The governing equations are obtained using energy functional with the Rayleigh-Ritz method. Results are presented on the frequency characteristics and the influences of constituent various volume fractions for Type I and II FG conical shells. the boundary conditions are simply supported.
[Amirhossein Nezhadi, Roslan Abdul Rahman, Amran Ayob. **Comparison of Two Kinds of Functionally Graded Conical Shells with Various Gradient Index for Vibration Analysis.** 2012;8(3):651-657]. (ISSN: 1545-1003). http://www.americanscience.org. 87

Keywords: Functionally Graded Materials, Conical shell, Rayleigh-Ritz Method, Energy Functional, Vibration.

Introduction

Conical shells have been widely utilized in a variety of engineering fields as important structural components due to their special geometric shapes, especially in marine industries and aerospace. Considerable investigations have been conducted to examine the dynamic responses of such structures. Leissa (1993) provided an earlier survey on the free vibration of conical shells, the effects of semi-vertex angles and different boundary conditions on the frequency characteristics of conical shells were investigated. The vibration analysis of shallow conical shells by a global Ritz formulation based on the energy principle is done by Liew and Lim 1994. Next, a formulation for the free vibration of moderately thick conical shell panels based on shear deformable theory was also presented by them (1995). He et al. (2002), Ng et al. (2002) and Liew et al. (2004) examined the finite element analysis of shell and shell panels subjected to vibration. The generalized differential quadrature method was employed to study the free vibration of composite laminated conical shells by Shu (1996), and the vibration characteristics of open conically curved, isotropic shell panels using a h–p version of finite element method was investigated by Bardell et al. (1998). A new kind of composite materials are known as functionally graded materials (FGM) that are formed by mixing two or more different materials according to a pre-determined formula that depends on the volume fractions of constituents. Such materials possess smooth and continuous material properties, which make them more suitable in engineering applications. Much effort has been used to various structural analyses of functionally graded structures, such as static, thermal stresses, vibration analyses and buckling. Noda (1999) presented a review on thermal stresses in functionally graded materials, the thermal stresses on the functionally graded plates and the thermal stress intensity factor in the functionally graded plates with crack were discussed. The stresses and strains in a functionally thick-walled tube under uniform thermal loading was examined by Fukui et al. (1993), and studied the effects of FGM materials on the parametric resonance of plate structures was studied by Ng et al. (2000). The thermal stress behavior of functionally graded hollow circular cylinders was investigated by Liew et al. (2003), and the static and dynamic response of functionally graded plates in terms of the combination of the first-order shear deformation plate theory and the von Kármán strains was examined by Praveen and Reddy (1998).

A finite element formulation for the active control of functionally graded plates with integrated piezoelectric actuators and sensors was provided by He et al. (2001), and the vibration analysis of variable thickness annular functionally graded plates was conducted by Efraim and Eisenberger (2007). A few publications on the analysis of functionally graded conical shells have been reported in literature. The stability of truncated conical shells of functionally

graded material subjected to external pressure was investigated by Sofiyev (2004). Tornabene (2009) was calculated free vibration analysis of moderately thick functionally graded conical, cylindrical shell and annular plate structures with a four-parameter power-law distribution. The formulation was based on generalized differential quadrature method and the first order shear deformation theory. Tornbene et al. (2009) also examined the same structures with two different power-law distributions. The applications of functionally graded conical shell can be very extensive. Due to their high strength and resistance to temperature change, the functionally graded conical shell can be applied to military aircraft propulsion system, fuselage structures of civil airliners, and other machine parts.

In this study, Rayleigh-Ritz method is used to comparison natural frequencies of two kinds of functionally graded conical shells with various gradient indexes.

2. Functionally gradient materials

In which for functionally graded materials with two constituent materials Poisson ratio υ is assumed to be constant through the thickness, whereas the variations through the thickness of Young's modulus $E(\eta)$ and the mass density per unit volume $\rho(\eta)$ can be written as (Matsunaga, 2009)

$$E(\eta) = E_2 + (E_1 - E_2)(0.5 + \frac{\eta}{h})^p \quad (1)$$

$$\rho(\eta) = \rho_2 + (\rho_1 - \rho_2)(0.5 + \frac{\eta}{h})^p \quad (2)$$

Where η is the thickness coordinate ($-h/2 \leq \eta \leq h/2$), and $p \geq 0$ is the gradient index. The material properties vary continuously from material 2 at the inner surface of the conical shell to material 1 at the outer surface of the conical shell.

3. Equation of motion of FG conical shell

A thin and FG conical shell with constant thickness is assumed. Fig. 1 shows the schematic diagram of the conical shell. The two boundaries of the conical shell are simply supported (S-S). The corresponding curvilinear surface coordinates $O - \xi\zeta\eta$ and Cartesian coordinates $O - xyz$ are also shown in Fig. 1. The curvilinear surface coordinates are limited to be orthogonal ones which coincide with the lines of principal curvature of the neutral surface. For conical shells, the lines of principal curvature of the neutral surface are the circles (ζ-axis) and parallel meridians (ξ-axis).

.

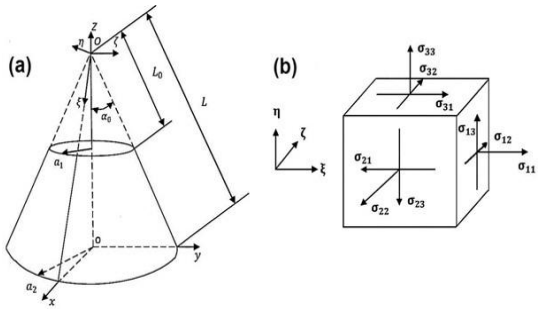

Fig. 1. The schematic diagram of a FGM conical shell (a) The geometry and the curvilinear surface and Cartesian Coordinate Systems; (b) the infinitesimal shell element and the corresponding stresses.

For a thin conical shell, plane stress condition is assumed and the constitutive relation is given by

$$\begin{Bmatrix} \sigma_{11} \\ \sigma_{22} \\ \sigma_{12} \\ \sigma_{23} \end{Bmatrix} = \begin{bmatrix} \frac{E(\eta)}{(1-\mu^2)} & \frac{\mu E(\eta)}{(1-\mu^2)} & 0 & 0 \\ \frac{\mu E(\eta)}{(1-\mu^2)} & \frac{E(\eta)}{(1-\mu^2)} & 0 & 0 \\ 0 & 0 & \frac{E(\eta)}{2(1+\mu)} & 0 \\ 0 & 0 & 0 & \frac{E(\eta)}{2(1+\mu)} \end{bmatrix} \times \begin{Bmatrix} \varepsilon_{11} \\ \varepsilon_{22} \\ \varepsilon_{12} \\ \varepsilon_{23} \end{Bmatrix} \quad (3)$$

where ε_{ij} $(i, j = 1, 2, 3)$ are the strains and σ_{ij} $(i, j = 1, 2, 3)$ are the stresses in which 1, 2 and 3 coincide with the ξ, ζ and η directions and $E(\eta)$ is the Young's modulus and μ is the Poisson's ratio. Where σ_{11} and σ_{22} are the normal stresses acting in the ξ and ζ directions, σ_{12} and σ_{23} are the shear stresses in the curvilinear coordinate $O - \xi\zeta\eta$ as shown in Fig. 1b. To determine the equation of motion of the conical shell, the Lagrangian function with the Rayleigh-Ritz method will be used. The Lagrangian function is written by (Soedel, 2004)

$$\int_{t_1}^{t_2} \delta(T - U)dt = 0 \quad (4)$$

Where T the kinetic energy, U strain energy and W work, t_1 and t_2 are the integration time limits, $\delta(0)$ denotes the first variation. The strain energy and kinetic energy and virtual work of a conical shell can be written as

$$T = \frac{1}{2}\int_{-h/2}^{h/2}\int_{0}^{2\pi}\int_{L_0}^{L}\rho(\eta)\left[\left(\frac{\partial u}{\partial t}\right)^2+\left(\frac{\partial v}{\partial t}\right)^2+\left(\frac{\partial w}{\partial t}\right)^2\right]\xi\sin\alpha_0\, d_\xi d_\zeta d_\eta \quad (5)$$

$$U = \frac{1}{2}\int_{-h/2}^{h/2}\int_{0}^{2\pi}\int_{L_0}^{L}(\sigma_{11}\varepsilon_{11}+\sigma_{22}\varepsilon_{22}+\sigma_{12}\varepsilon_{12}+\sigma_{23}\varepsilon_{23})\xi\sin\alpha_0\, d_\xi d_\zeta d_\eta \quad (6)$$

For simply supported conical shell, the boundary conditions at both ends can be written as

$$v = w = N_{11} = M_{11} = 0 \quad (7)$$

at $\xi = l$ and $\xi = l_0$ would be considered. The displacement fields which satisfy these boundary conditions can be written as

$$u(\xi,\zeta,t) = \cos\left[\frac{i\pi(\xi-l_0)}{l-l_0}\right]\cos(j\zeta)\, p(t) \quad (8)$$

$$v(\xi,\zeta,t) = \sin\left[\frac{i\pi(\xi-l_0)}{l-l_0}\right]\sin(j\zeta)\, r(t) \quad (9)$$

$$w(\xi,\zeta,t) = \sin\left[\frac{i\pi(\xi-l_0)}{l-l_0}\right]\cos(j\zeta)\, s(t) \quad (10)$$

$i = 1,2,\dots,m\,;\quad j = 1,2,\dots,n,$

where i and j denote the wave numbers in the meridional and circumferential directions and p, r, s are the generalized coordinates or modal coordinates. Substituting Eqs. (5) and (6) in terms of the displacement fields into Eq. (4) and fulfilling the variation operation in terms of p, r and s. They can be obtained as

$$M_t\frac{d^2X}{dt^2} + K_tX = 0 \quad (11)$$

where M_t the generalized mass matrix, K_t the stiffness matrix, X the generalized coordinate matrix and written by

$$M_t = \begin{bmatrix} M_1 & 0 & 0 \\ 0 & M_2 & 0 \\ 0 & 0 & M_3 \end{bmatrix} \qquad K_t = \begin{bmatrix} K_1 & K_2 & K_3 \\ K_2^T & K_4 & K_5 \\ K_3^T & K_5^T & K_6 \end{bmatrix}$$

$$X = [p^T \;\; r^T \;\; s^T]^T \quad (12)$$

where M_1, M_2 and M_3 are the modal mass matrices and $K_1, K_2, \dots, K_6$ are the modal stiffness matrices which are given in Appendix A. A solution of Eq. (11) is in the form

$$X(t) = X_0 e^{\lambda t} \quad (13)$$

where λ is the characteristic values or the eigenvalue and X_0 is the eigenvector. Substituting Eq. (13) into the homogeneous differential equation of Eq. (11) leads to the following standard eigenvalue problem:

$$(M_t\lambda^2 + K_t)X_0 = 0 \quad (14)$$

From which the eignvalues and eignvectors can be obtinethed. The imaginary parts of the eigenvalues are the natural frequencies of the FG conical shell.

4. Results and discussions

The results for Metal are compared with the open literature in Table 1. In the numerical calculations, the non-dimensional frequency parameter is defined as ((Lam and Li, 1999) ; (Liew et al., 2002))

$$f = \omega_0\alpha_2\sqrt{\frac{\rho_m(1-\mu^2)}{E_m}} \quad (15)$$

where ω_0 is the natural frequency of the conical shell in radians per second. The material properties used in the present study is:

Metal (Aluminium, Al): $E_M = 70$ GPa, $\rho_M = 2710\ kg/m^3$, $\mu = 0.3$

Ceramic (Almina, Al_2O_3): $E_C = 380$ GPa, $\rho_C = 3800\ kg/m^3$, $\mu = 0.3$

The variation through the thickness of Young's modulus $E(\eta)$ and mass density per unit volume $\rho(\eta)$ are the same as Eqs. (1) and (2). The structural parameters are $h = 0.004$ m, $h/a_2 = 0.01$, $(L - L_0)\sin\alpha_0/a_2 = 0.25$. For metal, the frequency parameters computed by Eq. (15) are listed in Table 1. Also the corresponding results by ((Lam and Li, 1999) ; (Irie et al., 1984)) are listed in Table 1.

The frequencies of two FG conical shells with two different FGM configurations are studied: Type I FG conical shell and Type II FG conical shell. Type I FG conical shell has aluminum on its inner surface and almina on its outer surface and Type II FG conical shell has almina on its inner surface and aluminum on its outer surface. Tables 2, 3 and 4 show the variations of the natural frequencies (Hz) with the circumferential wave numbers n for a Type I FG conical shell. The columns P^C and P^M show the natural frequencies for a ceramic conical shell and a metal conical shell, respectively. The effects of changing gradient index (P) can be seen from tables. As P increased, the natural frequencies decreased. When P is small, the natural frequencies approached those of P^C and when P is large they approached those of P^M. Hence, the natural frequencies for $P > 0$ fell between those of P^C and P^M for a given circumferential wave number n.

Table 1. Comparisons of frequency parameter f for the conical shell with S-S boundaries (m = 1, Metal).

	n	Irie et al (1984)	Lam and Li (1999)	Present
$\alpha_0 = 30^0$	2	0.7910	0.8420	0.84307
	3	0.7284	0.7376	0.74163
	4	0.6352	0.6362	0.64194
	5	0.5531	0.5528	0.55902
	6	0.4949	0.4950	0.50079
	7	0.4653	0.4661	0.47079
	8	0.4654	0.4660	0.46921
	9	0.4892	0.4916	0.49318
$\alpha_0 = 45^0$	2	0.6879	0.7655	0.76424
	3	0.6973	0.7212	0.72108
	4	0.6664	0.6739	0.67467
	5	0.6304	0.6323	0.63364
	6	0.6032	0.6035	0.60492
	7	0.5918	0.5921	0.59311
	8	0.5992	0.6001	0.60045
	9	0.6257	0.6273	0.62691
$\alpha_0 = 60^0$	2	0.5772	0.6348	0.63423
	3	0.6001	0.6238	0.62361
	4	0.6054	0.6145	0.61459
	5	0.6077	0.6111	0.61128
	6	0.6159	0.6171	0.61721
	7	0.6343	0.6350	0.63479
	8	0.6650	0.6660	0.66525
	9	0.7084	0.7101	0.70873

Table 2. Variation of natural frequencies (Hz) against circumferential wave number n (m=1).

Type I FG conical shell $\alpha = 30^0$						
n	P^C	P=1	P=3	P=8	P=30	P^M
1	3847	3193	2702	2338	2079	1955
2	3516	2917	2469	2138	1901	1787
3	3093	2563	2171	1883	1675	1572
4	2677	2213	1877	1633	1453	1360
5	2331	1918	1630	1428	1272	1185
6	2088	1704	1454	1288	1150	1061
7	1963	1582	1358	1222	1094	998
8	1957	1554	1343	1230	1104	994
9	2057	1612	1401	1304	1173	1045
10	2247	1742	1521	1433	1292	1142

Table 3. Variation of natural frequencies (Hz) against circumferential wave number n (m=1).

Type I FG conical shell $\alpha = 45^0$						
n	P^C	P=1	P=3	P=8	P=30	P^M
1	3316	2737	2322	2024	1802	1686
2	3187	2628	2230	1947	1734	1620
3	3007	2474	2102	1841	1640	1528
4	2814	2305	1962	1728	1541	1430
5	2642	2152	1837	1631	1456	1343
6	2523	2037	1746	1566	1401	1282
7	2473	1977	1702	1547	1387	1257
8	2504	1980	1713	1578	1417	1272
9	2615	2046	1779	1658	1492	1329
10	2799	2172	1896	1784	1608	1422

Table 4. Variation of natural frequencies (Hz) against circumferential wave number n (m=1).

Type I FG Conical Shell $\alpha = 60^0$						
n	P^C	P=1	P=3	P=8	P=30	P^M
1	2679	2175	1859	1657	1480	1362
2	2645	2142	1833	1638	1464	1344
3	2601	2099	1799	1615	1445	1321
4	2563	2057	1768	1598	1431	1302
5	2549	2032	1752	1597	1432	1295
6	2574	2036	1762	1621	1456	1308
7	2647	2078	1804	1676	1507	1345
8	2774	2162	1883	1764	1589	1410
9	2955	2289	2000	1887	1701	1502
10	3189	2456	2152	2041	1842	1621

Tables 5, 6 and 7 show the alterations of the natural frequencies (Hz) with the circumferential wave numbers n for a Type II FG conical shell.

Table 5. Variation of natural frequencies (Hz) against circumferential wave number n (m=1).

Type II FG conical shell $\alpha = 30^0$						
n	P^C	P=15	P=8	P=5	P=3	P^M
1	3847	3779	3725	3661	3558	1955
2	3516	3453	3403	3344	3250	1787
3	3093	3036	2991	2938	2855	1572
4	2677	2624	2583	2536	2463	1360
5	2331	2279	2241	2198	2133	1185
6	2088	2033	1994	1952	1892	1061
7	1963	1899	1857	1813	1754	998
8	1957	1879	1830	1783	1721	994
9	2057	1964	1907	1851	1783	1045
10	2247	2135	2067	2004	1928	1142

.

The influence of the gradient index (P) on the natural frequencies is the opposite of a Type I FG conical shell. Unlike a Type I FG conical shell where the natural frequencies decreased with P, the natural frequencies for a Type II FG conical shell increased with P. Thus the influence of the gradient index for a Type II FG conical shell is different from a Type I FG conical shell.

Table 6. Variation of natural frequencies (Hz) against circumferential wave number n (m=1).

Type II FG conical shell $\alpha = 45^0$						
n	P^C	P=15	P=8	P=5	P=3	P^M
1	3316	3248	3197	3138	3048	1686
2	3187	3120	3070	3013	2926	1620
3	3007	2940	2891	2836	2753	1528
4	2814	2746	2697	2643	2564	1430
5	2642	2571	2521	2468	2392.3	1343
6	2523	2444	2391	2337	2262.6	1282
7	2473	2384	2327	2270	2193.5	1257
8	2504	2401	2337	2274	2194.3	1272
9	2615	2495	2422	2352	2266.0	1329
10	2799	2661	2577	2500	2405.0	1422

Table 7. Variation of natural frequencies (Hz) against circumferential wave number n (m=1).

Type II FG conical shell $\alpha = 60^0$						
n	P^C	P=15	P=8	P= 5	P=3	P^M
1	2679	2603	2551.4	2496	2418	1362
2	2645	2566.9	2514.2	2458	2381	1344
3	2601	2519.1	2464.9	2408	2331	1321
4	2563	2476.0	2419.3	2361	2283	1302
5	2549	2454.4	2393.9	2333	2254	1295
6	2574	2468.9	2403.3	2339	2256	1308
7	2647	2529.8	2457.5	2388	2301	1345
8	2774	2642.1	2561.9	2486	2392	1410
9	2955	2806.9	2717.6	2634	2532	1502
10	3189	3022.2	2922.2	2829	2719	1621

5. Conclusions

A study on the vibration of functionally graded (FG) conical shells made of aluminum and almina has been presented. The study was done for two kinds of functionally graded conical shells where the configurations of the constituent materials in the functionally graded conical shells are different. Type I FG conical shell has aluminum on its inner surface and almina on its outer surface and Type II FG conical shell has almina on its inner surface and aluminum on its outer surface. One is named as a Type I FG conical shell and has properties that change continuously from aluminum on its inner surface to almina on its outer surface. The other is named as a Type II FG cylindrical shell and has properties that change continuously from almina on its inner surface to aluminum on its outer surface. The analysis was done by Rayleigh-Ritz method. For validation, the results are compared with those in the literature and have found to be accurate. The influence of the gradient index (P) on the frequencies for Types I and II FG conical shells has been found to be different. For the Type I FG conical shells, the natural frequencies decreased when (P) increased, and for the Type II FG conical shells, the natural frequencies increased when P increased. In Types I and II FG conical shells, the natural frequencies for all values of P are between those for aluminum and almina conical shells. Therefore, the gradient index and the configurations of the constituent materials affect the natural frequencies.

Appendix A. The expressions of the modal mass, modal stiffness and forcing matrices in Eqs. (11) are given by

$$M_1 = \sin\alpha_0 \int_0^{2\pi}\int_{l_0}^{l}\int_{-h/2}^{h/2} UU^T \rho(\eta)\xi d\eta d\xi d\zeta$$

$$M_2 = \sin\alpha_0 \int_0^{2\pi}\int_{l_0}^{l}\int_{-h/2}^{h/2} VV^T \rho(\eta)\xi d\eta d\xi d\zeta$$

$$M_3 = \sin\alpha_0 \int_0^{2\pi}\int_{l_0}^{l}\int_{-h/2}^{h/2} WW^T \rho(\eta)\xi d\eta d\xi d\zeta$$

$$K_1 = \frac{\sin\alpha_0}{1-\mu^2}\int_0^{2\pi}\int_{l_0}^{l}\int_{-h/2}^{h/2}\left(\frac{\partial U}{\partial\xi}\frac{\partial U^T}{\partial\xi}\xi + UU^T\frac{1}{\xi} + \mu\frac{\partial U}{\partial\xi}U^T + \mu U\frac{\partial U^T}{\partial\xi}\right)E(\eta)d\eta d\xi d\zeta + \frac{1}{\sin\alpha_0}\int_0^{2\pi}\int_{l_0}^{l}\int_{-h/2}^{h/2}\frac{\partial U}{\partial\zeta}\frac{\partial U^T}{\partial\zeta}\frac{1}{\xi}G(\eta)d\eta d\xi d\zeta$$

$$K_2 = \frac{1}{1-\mu^2}\int_0^{2\pi}\int_{l_0}^{l}\int_{-h/2}^{h/2}\left(U\frac{\partial V^T}{\partial\zeta}\frac{1}{\xi} + \mu\frac{\partial U}{\partial\xi}\frac{\partial V^T}{\partial\zeta}\right)E(\eta)d\eta d\xi d\zeta + \frac{1}{2(1+\mu)}\int_0^{2\pi}\int_{l_0}^{l}\int_{-h/2}^{h/2}\left(\frac{\partial U}{\partial\zeta}\frac{\partial V^T}{\partial\xi} - \frac{\partial U}{\partial\zeta}V^T\frac{1}{\xi}\right)E(\eta)d\eta d\xi d\zeta + \frac{\mu}{(1-\mu^2)\tan\alpha_0}\int_0^{2\pi}\int_{l_0}^{l}\int_{-h/2}^{h/2}\left(\frac{\partial U}{\partial\xi}\right)\left(\frac{\partial V^T}{\partial\zeta}\right)\frac{E(\eta)\eta}{\xi}d\eta d\xi d\zeta + \frac{1}{(1-\mu^2)\tan\alpha_0}\int_0^{2\pi}\int_{l_0}^{l}\int_{-h/2}^{h/2}(U)\left(\frac{\partial V^T}{\partial\zeta}\right)\frac{E(\eta)\eta}{\xi^2}d\eta d\xi d\zeta + \frac{1}{2(1+\mu)\tan\alpha_0}\int_0^{2\pi}\int_{l_0}^{l}\int_{-h/2}^{h/2}\left(\frac{\partial U}{\partial\zeta}\right)\left(\frac{\partial V^T}{\partial\xi}\right)\frac{E(\eta)\eta}{\xi}d\eta d\xi d\zeta - \frac{2}{2(1+\mu)\tan\alpha_0}\int_0^{2\pi}\int_{l_0}^{l}\int_{-h/2}^{h/2}\left(\frac{\partial U}{\partial\zeta}\right)(V^T)\frac{E(\eta)\eta}{\xi^2}d\eta d\xi d\zeta$$

$$K_3 = \frac{\cos\alpha_0}{1-\mu^2}\int_0^{2\pi}\int_{l_0}^{l}\int_{-h/2}^{h/2}(UW^T\frac{1}{\xi}+\mu\frac{\partial U}{\partial\xi}W^T)E(\eta)d\eta d\xi d\zeta$$
$$-\frac{\sin\alpha_0}{(1-\mu^2)}\int_0^{2\pi}\int_{l_0}^{l}\int_{-h/2}^{h/2}\left(\frac{\partial U}{\partial\xi}\right)\left(\frac{\partial^2 W^T}{\partial\xi^2}\right)E(\eta)\eta\xi d\eta d\xi d\zeta$$
$$-\frac{\mu\sin\alpha_0}{(1-\mu^2)\sin^2\alpha_0}\int_0^{2\pi}\int_{l_0}^{l}\int_{-h/2}^{h/2}\left(\frac{\partial U}{\partial\xi}\right)\left(\frac{\partial^2 W^T}{\partial\zeta^2}\right)\frac{E(\eta)\eta}{\xi}d\eta d\xi d\zeta$$
$$-\frac{\mu\sin\alpha_0}{(1-\mu^2)}\int_0^{2\pi}\int_{l_0}^{l}\int_{-h/2}^{h/2}\left(\frac{\partial U}{\partial\xi}\right)\left(\frac{\partial W^T}{\partial\xi}\right)E(\eta)\eta d\eta d\xi d\zeta$$
$$-\frac{1}{(1-\mu^2)\sin\alpha_0}\int_0^{2\pi}\int_{l_0}^{l}\int_{-h/2}^{h/2}(U)\left(\frac{\partial^2 W^T}{\partial\zeta^2}\right)\frac{E(\eta)\eta}{\xi^2}d\eta d\xi d\zeta$$
$$-\frac{\sin\alpha_0}{(1-\mu^2)}\int_0^{2\pi}\int_{l_0}^{l}\int_{-h/2}^{h/2}(U)\left(\frac{\partial W^T}{\partial\xi}\right)\frac{E(\eta)\eta}{\xi}d\eta d\xi d\zeta$$
$$-\frac{\mu\sin\alpha_0}{(1-\mu^2)}\int_0^{2\pi}\int_{l_0}^{l}\int_{-h/2}^{h/2}(U)\left(\frac{\partial^2 W^T}{\partial\xi^2}\right)E(\eta)\eta d\eta d\xi d\zeta$$
$$-\frac{2}{2(1+\mu)\sin\alpha_0}\int_0^{2\pi}\int_{l_0}^{l}\int_{-h/2}^{h/2}\left(\frac{\partial U}{\partial\zeta}\right)\left(\frac{\partial^2 W^T}{\partial\xi\partial\zeta}\right)\frac{E(\eta)\eta}{\xi}d\eta d\xi d\zeta$$
$$+\frac{2}{2(1+\mu)\sin\alpha_0}\int_0^{2\pi}\int_{l_0}^{l}\int_{-h/2}^{h/2}\left(\frac{\partial U}{\partial\zeta}\right)\left(\frac{\partial W^T}{\partial\zeta}\right)\frac{E(\eta)\eta}{\xi^2}d\eta d\xi d\zeta$$
$$K_4 = \frac{1}{(1-\mu^2)\sin\alpha_0}\int_0^{2\pi}\int_{l_0}^{l}\int_{-h/2}^{h/2}\left(\frac{\partial V}{\partial\zeta}\frac{\partial V^T}{\partial\zeta}\frac{1}{\xi}\right.$$
$$\left.+\frac{\eta^2}{\tan^2\alpha_0}\frac{\partial V}{\partial\zeta}\frac{\partial V^T}{\partial\zeta}\frac{1}{\xi^3}\right)E(\eta)d\eta d\xi d\zeta$$
$$+\sin\alpha_0\int_0^{2\pi}\int_{l_0}^{l}\int_{-h/2}^{h/2}\left(\frac{\partial V}{\partial\xi}\frac{\partial V^T}{\partial\xi}\xi+VV^T\frac{1}{\xi}\right.$$
$$\left.-\frac{\partial V}{\partial\xi}V^T-V\frac{\partial V^T}{\partial\xi}\right)G(\eta)d\eta d\xi d\zeta+\frac{\sin\alpha_0}{\tan^2\alpha_0}\times$$
$$\int_0^{2\pi}\int_{l_0}^{l}\int_{-h/2}^{h/2}\left(VV^T\frac{1}{\xi}+\eta^2\left(\frac{\partial V}{\partial\xi}\frac{\partial V^T}{\partial\xi}\frac{1}{\xi}+4VV^T\frac{1}{\xi^3}-2\frac{\partial V}{\partial\xi}V^T\frac{1}{\xi^2}-2V\frac{\partial V^T}{\partial\xi}\frac{1}{\xi^2}\right)\right)$$
$$G(\eta)d\eta d\xi d\zeta+$$
$$\frac{2}{(1-\mu^2)\sin\alpha_0\tan\alpha_0}\int_0^{2\pi}\int_{l_0}^{l}\int_{-h/2}^{h/2}\left(\frac{\partial V}{\partial\zeta}\right)\left(\frac{\partial V^T}{\partial\zeta}\right)\frac{E(\eta)\eta}{\xi^2}d\eta d\xi d\zeta$$
$$+\frac{2\cos\alpha_0}{2(1+\mu)}\int_0^{2\pi}\int_{l_0}^{l}\int_{-h/2}^{h/2}\left(\frac{\partial V}{\partial\xi}\right)\left(\frac{\partial V^T}{\partial\xi}\right)E(\eta)\eta d\eta d\xi d\zeta$$
$$-\frac{3\cos\alpha_0}{2(1+\mu)}\int_0^{2\pi}\int_{l_0}^{l}\int_{-h/2}^{h/2}\left(\frac{\partial V}{\partial\xi}\right)(V^T)\frac{E(\eta)\eta}{\xi}d\eta d\xi d\zeta$$
$$-\frac{3\cos\alpha_0}{2(1+\mu)}\int_0^{2\pi}\int_{l_0}^{l}\int_{-h/2}^{h/2}(V)\left(\frac{\partial V^T}{\partial\xi}\right)\frac{E(\eta)\eta}{\xi}d\eta d\xi d\zeta$$
$$+\frac{4\cos\alpha_0}{2(1+\mu)}\int_0^{2\pi}\int_{l_0}^{l}\int_{-h/2}^{h/2}(V)(V^T)\frac{E(\eta)\eta}{\xi^2}d\eta d\xi d\zeta$$
$$K_5 = \frac{1}{(1-\mu^2)\tan\alpha_0}\int_0^{2\pi}\int_{l_0}^{l}\int_{-h/2}^{h/2}\frac{\partial V}{\partial\zeta}\frac{W^T}{\xi}E(\eta)d\eta d\xi d\zeta$$
$$-\frac{1}{(1-\mu^2)\tan\alpha_0}\int_0^{2\pi}\int_{l_0}^{l}\int_{-h/2}^{h/2}\left(\frac{\partial V}{\partial\zeta}\frac{\partial W^T}{\partial\xi}\frac{1}{\xi^2}+\mu\frac{\partial V}{\partial\zeta}\frac{\partial^2 W^T}{\partial\xi^2}\frac{1}{\xi}+\right.$$
$$\left.\frac{1}{\sin^2\alpha_0}\frac{\partial V}{\partial\zeta}\frac{\partial^2 W^T}{\partial\zeta^2}\frac{1}{\xi^3}\right)E(\eta)\eta^2 d\eta d\xi d\zeta+$$
$$\frac{2}{\tan\alpha_0}\int_0^{2\pi}\int_{l_0}^{l}\int_{-h/2}^{h/2}\left(\frac{\partial V}{\partial\xi}\frac{\partial W^T}{\partial\zeta}\frac{1}{\xi^2}-\frac{\partial V}{\partial\xi}\frac{\partial^2 W^T}{\partial\xi\partial\zeta}\frac{1}{\xi}+\frac{2V}{\xi^2}\frac{\partial^2 W^T}{\partial\xi\partial\zeta}-\right.$$
$$\left.\frac{2V}{\xi^3}\frac{\partial W^T}{\partial\zeta}\right)G(\eta)\eta^2 d\eta d\xi d\zeta+\frac{1}{(1-\mu^2)\tan^2\alpha_0}\times$$
$$\int_0^{2\pi}\int_{l_0}^{l}\int_{-h/2}^{h/2}\left(\frac{\partial V}{\partial\zeta}\right)(W^T)\frac{E(\eta)\eta}{\xi^2}d\eta d\xi d\zeta$$
$$-\frac{1}{(1-\mu^2)\sin^2\alpha_0}\int_0^{2\pi}\int_{l_0}^{l}\int_{-h/2}^{h/2}\left(\frac{\partial V}{\partial\zeta}\right)\left(\frac{\partial^2 W^T}{\partial\zeta^2}\right)\frac{E(\eta)\eta}{\xi^2}d\eta d\xi d\zeta$$
$$-\frac{1}{(1-\mu^2)}\int_0^{2\pi}\int_{l_0}^{l}\int_{-h/2}^{h/2}\left(\frac{\partial V}{\partial\zeta}\right)\left(\frac{\partial W^T}{\partial\xi}\right)\frac{E(\eta)\eta}{\xi}d\eta d\xi d\zeta$$
$$-\frac{\mu}{(1-\mu^2)}\int_0^{2\pi}\int_{l_0}^{l}\int_{-h/2}^{h/2}\left(\frac{\partial V}{\partial\zeta}\right)\left(\frac{\partial^2 W^T}{\partial\xi^2}\right)E(\eta)\eta d\eta d\xi d\zeta$$
$$-\frac{2}{2(1+\mu)}\int_0^{2\pi}\int_{l_0}^{l}\int_{-h/2}^{h/2}\left(\frac{\partial V}{\partial\xi}\right)\left(\frac{\partial^2 W^T}{\partial\xi\partial\zeta}\right)E(\eta)\eta d\eta d\xi d\zeta$$
$$+\frac{2}{2(1+\mu)\sin\alpha_0}\int_0^{2\pi}\int_{l_0}^{l}\int_{-h/2}^{h/2}\left(\frac{\partial V}{\partial\xi}\right)\left(\frac{\partial W^T}{\partial\zeta}\right)\frac{E(\eta)\eta}{\xi^2}d\eta d\xi d\zeta$$
$$+\frac{2}{2(1+\mu)}\int_0^{2\pi}\int_{l_0}^{l}\int_{-h/2}^{h/2}(V)\left(\frac{\partial^2 W^T}{\partial\xi\partial\zeta}\right)\frac{E(\eta)\eta}{\xi}d\eta d\xi d\zeta$$
$$-\frac{2}{2(1+\mu)}\int_0^{2\pi}\int_{l_0}^{l}\int_{-h/2}^{h/2}(V)\left(\frac{\partial W^T}{\partial\zeta}\right)\frac{E(\eta)\eta}{\xi^2}d\eta d\xi d\zeta$$
$$K_6 = \frac{\sin\alpha_0}{(1-\mu^2)}\int_0^{2\pi}\int_{l_0}^{l}\int_{-h/2}^{h/2}\left(\frac{\partial^2 W}{\partial\xi^2}\frac{\partial^2 W^T}{\partial\xi^2}\xi+\frac{\partial W}{\partial\xi}\frac{\partial W^T}{\partial\xi}\frac{1}{\xi}+\right.$$
$$\left.\mu\frac{\partial^2 W}{\partial\xi^2}\frac{\partial W^T}{\partial\xi}+\mu\frac{\partial W}{\partial\xi}\frac{\partial^2 W^T}{\partial\xi^2}\right)E(\eta)\eta^2 d\eta d\xi d\zeta$$
$$+\frac{1}{(1-\mu^2)\sin\alpha_0}\int_0^{2\pi}\int_{l_0}^{l}\int_{-h/2}^{h/2}\left(\frac{1}{\sin^2\alpha_0}\frac{\partial^2 W}{\partial\zeta^2}\frac{\partial^2 W^T}{\partial\zeta^2}\frac{1}{\xi^3}\right.$$
$$\left.+\mu\frac{\partial^2 W}{\partial\xi^2}\frac{\partial^2 W^T}{\partial\zeta^2}\frac{1}{\xi}+\mu\frac{\partial^2 W}{\partial\zeta^2}\frac{\partial^2 W^T}{\partial\xi^2}\frac{1}{\xi}+\frac{\partial^2 W}{\partial\zeta^2}\frac{\partial W^T}{\partial\xi}\frac{1}{\xi^2}+\frac{\partial W}{\partial\xi}\frac{\partial^2 W^T}{\partial\zeta^2}\frac{1}{\xi^2}\right)$$
$$E(\eta)\eta^2 d\eta d\xi d\zeta$$
$$+\frac{\sin\alpha_0}{(1-\mu^2)\tan^2\alpha_0}\int_0^{2\pi}\int_{l_0}^{l}\int_{-h/2}^{h/2}\frac{WW^T}{\xi}E(\eta)d\eta d\xi d\zeta+$$
$$\frac{4}{\sin\alpha_0}\int_0^{2\pi}\int_{l_0}^{l}\int_{-h/2}^{h/2}\left(\frac{\partial^2 W}{\partial\xi\partial\zeta}\frac{\partial^2 W^T}{\partial\xi\partial\zeta}\xi+\frac{\partial W}{\partial\zeta}\frac{\partial W^T}{\partial\zeta}\frac{1}{\xi}-\frac{\partial^2 W}{\partial\xi\partial\zeta}\frac{\partial W^T}{\partial\zeta}\right.$$
$$\left.-\frac{\partial W}{\partial\zeta}\frac{\partial^2 W^T}{\partial\xi\partial\zeta}\right)\frac{G(\eta)}{\xi^2}\eta^2 d\eta d\xi d\zeta-\frac{1}{(1-\mu^2)\sin\alpha_0\tan\alpha_0}\times$$
$$\int_0^{2\pi}\int_{l_0}^{l}\int_{-h/2}^{h/2}\left(\frac{\partial^2 W}{\partial\zeta^2}\right)(W^T)\frac{E(\eta)\eta}{\xi^2}d\eta d\xi d\zeta$$
$$-\frac{\cos\alpha_0}{(1-\mu^2)}\int_0^{2\pi}\int_{l_0}^{l}\int_{-h/2}^{h/2}\left(\frac{\partial W}{\partial\xi}\right)(W^T)\frac{E(\eta)\eta}{\xi}d\eta d\xi d\zeta$$
$$-\frac{\mu\cos\alpha_0}{(1-\mu^2)}\int_0^{2\pi}\int_{l_0}^{l}\int_{-h/2}^{h/2}\left(\frac{\partial^2 W}{\partial\xi^2}\right)(W^T)E(\eta)\eta d\eta d\xi d\zeta$$
$$-\frac{1}{(1-\mu^2)\sin\alpha_0\tan\alpha_0}\int_0^{2\pi}\int_{l_0}^{l}\int_{-h/2}^{h/2}(W)\left(\frac{\partial^2 W^T}{\partial\zeta^2}\right)\frac{E(\eta)\eta}{\xi^2}$$
$$d\eta d\xi d\zeta$$
$$-\frac{\cos\alpha_0}{(1-\mu^2)}\int_0^{2\pi}\int_{l_0}^{l}\int_{-h/2}^{h/2}(W)\left(\frac{\partial W^T}{\partial\xi}\right)\frac{E(\eta)\eta}{\xi}d\eta d\xi d\zeta$$
$$-\frac{\mu\cos\alpha_0}{(1-\mu^2)}\int_0^{2\pi}\int_{l_0}^{l}\int_{-h/2}^{h/2}(W)\left(\frac{\partial^2 W^T}{\partial\xi^2}\right)E(\eta)\eta d\eta d\xi d\zeta \quad (16)$$

Acknowledgements:

Authors are grateful to the Universiti Teknologi Malaysia (Johor Bahru) for International Doctoral Fellowship (IDF) to carry out this research.

Corresponding Author:
Amirhossein Nezhadi
Faculty of Mechanical Engineering
Universiti Teknologi Malaysia (UTM)
81310 UTM Skudai, Johor, Malaysia.
E-mail: a_h_nezhadi@yahoo.com

References:

1. Leissa A. Vibration of shells. The Acoustic Society of America, 1993.
2. Liew KM, Lim CW. Vibratory characteristics of cantilevered rectangular shallow shells of variable thickness. AIAA J 1994; 32:387–96.
3. Liew KM, Lim CW. Vibration of perforated doubly-curved shallow shells with rounded corners. Int J Solids Struct 1994; 31:1519–36.
4. Lim CW, Liew KM. Vibratory behaviour of shallow conical shells by a global Ritz formulation. Eng Struct 1995; 17:63–9.
5. Lim CW, Liew KM. A higher order theory for vibration of shear deformable cylindrical shallow shells. Int J Mech Sci 1995; 37:277–95.
6. He XQ, Liew KM, Ng TY, Sivashanker SA. FEM model for the active control of curved FGM shells using piezoelectric sensor/actuator layers. Int J Numer Methods Eng 2002; 54:853–70.
7. Ng TY, He XQ, Liew KM. Finite element modeling of active control of functionally graded shells in frequency domain via piezoelectric sensors and actuators. Comput Mech2002;28:1–9.
8. Liew KM, He XQ, Kitipornchai S. Finite element method for the feedback control of FGM shells in the frequency domain via piezoelectric sensors and actuators. Comput Methods Appl Mech Eng 2004;193:257–73.
9. Shu C. Free vibration analysis of composite laminated conical shells by generalized differential quadrature. J Sound Vib 1996; 194:587–604.
10. Bardell NS, Dunsdon JM, Langley RS. Free vibration of thin, isotropic, open, conical panels. J Sound Vib 1998; 217:297–320.
11. Noda N. Thermal stresses in functionally graded materials. J Thermal Stress 1999; 22:477–512.
12. Fukui Y, Yamanaka N, Wakashima K. The stresses and strains in a thick-walled tube for functionally graded under uniform thermal loading. Int J Jpn Soc Mech Eng Ser A 1993 ; 36:156–62.
13. Ng TY, Lam KY, Liew KM. Effects of FGM materials on the parametric resonance of plate structures. Comput Methods Appl Mech Eng 2000;190:953–62.
14. Liew KM, Kitipornchai S, Zhang XZ, Lim CW. Analysis of the thermal stress behavior of functionally graded hollow circular cylinders. Int J Solids Struct 2003; 40:2355–80.
15. Praveen GN, Reddy JN. Nonlinear transient thermoelastic analysis of functionally graded ceramic–metal plates. Int J Solids Struct 1998; 33:4457–76.
16. He XQ, Ng TY, Sivashanker S, Liew KM. Active control of FGM plates with integrated piezoelectric sensors and actuators. Int J Solids Struct 2001; 38:1641–55.
17. Efraim E, Eisenberger M. Exact vibration analysis of variable thickness thick annular isotropic and FGM plates. J Sound Vib 2007; 299:720–38.
18. Sofiyev AH. The stability of functionally graded truncated conical shells subjected to aperiodic impulsive loading. Int J Solids Struct 2004; 41:3411–24.
19. Sofiyev AH. The vibration and stability behavior of freely supported FGM conical shells subjected to external pressure. Compos Struct 2009; 89:356–66.
20. Tornabene F. Free vibration analysis of functionally graded conical, cylindrical shell and annular plate structures with a four-parameter power-law distribution. Comput Methods Appl Mech Eng 2009; 198:2911–35.
21. Tornabene F, Viola E, Inman DJ. 2-D differential quadrature solution for vibration analysis of functionally graded conical, cylindrical shell and annular plate structures. J Sound Vib 2009; 328:259–90.
22. Matsunaga H. Free vibration and stability of functionally graded circular cylindrical shell according to a 2D higher -order shear deformation theory, Compos. Struct. 2009; (88) 519–31.
23. Soedel W. Vibrations of Shells and Plates, third ed. Marcel Dekker Inc., New York, USA, 2004.
24. Lam KY and Li H. Influence of boundary conditions on the frequency characteristics of a rotating truncated circular conical shell, *J.* Sound and Vib. 1999, (223) 171–95.
25. Liew KM and He XQ and Ng TY and Kitipornchai S. Active control of FGM shell subjected to a temperature gradient via piezoelectric sensor/actuator patches. Int. J. Numer. Meth. Engng. 2002; (55) 653–668.
26. Irie T and Yamada G and Tanaka K. Natural frequencies of truncated conical shells, *J. Sound Vib.* 1984; (92) 447–53.

3/2/2012